*Supplementary data for*

# AIPE-Active Neutral Ir(III) Complexes as Bi-Responsive Luminescent Chemosensors for Sensing Picric Acid and Fe$^{3+}$ in Aqueous Media

Qinglong Zhang[1,†], Jiangchao Xu[1,†], Qiang Xu[2,*], Chun Liu[1,*]

[1] State Key Laboratory of Fine Chemicals, Frontier Science Center for Smart Materials, School of Chemical Engineering, Dalian University of Technology, Linggong Road 2, Dalian 116024, China; E-mail: cliu@dlut.edu.cn.

[2] Instrumental Analysis Center, Dalian University of Technology, Dalian 116024, China; E-mail: qiangxu@dlut.edu.cn.

# Contents

## Materials and Instruments

Unless otherwise stated, the reagents and solvents were purchased from commercial suppliers and used as received. Cyclometalating ligands (**L1-L3**) were prepared following the methods reported in [1].^{1}H NMR and ^{13}C NMR spectra were recorded on a 400 MHz Varian Unity Inova spectrometer. The mass spectra were recorded with a MALDI micro MX spectrometer. The absorption spectra were recorded utilizing a PerkinElmer Lambda 1050+ UV-vis spectrophotometer. The emission spectra were recorded utilizing a HITACHI F-7100 fluorescence spectrophotometer. The photoluminescence quantum yields ($\Phi_{PL}$) were measured relative to [Ir(ppy)$_2$(acac)] ($\Phi_{PL}$ = 0.34 in $CH_2Cl_2$, under deoxygenated conditions). The phosphorescence decay traces were measured by employing an Edinburgh FLS920 spectrometer in a degassed $CH_2Cl_2$ solution and FLS1000 photoluminescence spectrometer in undeoxygenated $H_2O$/THF. Dynamic light scattering (DLS) was measured on Malvern ZS90. Density functional theory (DFT) calculations were conducted using B3LYP floods. The 6-31G basis sets were applied for C, H, and O atoms, while the LanL2DZ basis set was utilized for iridium atoms. All computations were executed using Gaussian 16.

## Characterization of Ir1-Ir3

**Ir1**. Yield: 72%; a yellow solid. ^{1}H NMR (400 MHz, CDCl$_3$) $\delta$ 8.70 (d, $J$ = 5.1 Hz, 1H), 8.32 (d, $J$ = 7.7 Hz, 1H), 8.13 (d, $J$ = 8.9 Hz, 1H), 8.07 (d, $J$ = 8.5 Hz, 1H), 8.02 - 7.96 (m, 1H), 7.87 - 7.67 (m, 11H), 7.58 - 7.35 (m, 14H), 7.17 (t, $J$ = 6.3 Hz, 1H), 6.97 (t, $J$ = 6.6 Hz, 1H), 5.77 (dd, $J$ = 9.9, 3.9 Hz, 1H), 5.61 (dd, $J$ = 9.9, 3.9 Hz, 1H). HRMS (MALDI-TOF, $m/z$): calcd. for C$_{52}$H$_{34}$F$_4$IrN$_3$O$_4$P$_2$ 1095.1590, found 1096.1715 ([M+H]$^+$), 1118.1535 ([M+Na]$^+$), 1134.1281 ([M+K]$^+$).

**Ir2**. Yield: 70%; a yellow solid. ^{1}H NMR (400 MHz, CDCl$_3$) $\delta$ 8.48 (s, 1H), 8.33 (d, $J$ = 7.6 Hz, 1H), 8.02 - 7.93 (m, 3H), 7.84 - 7.69 (m, 9H), 7.56 - 7.40 (m, 15H), 7.09 (s, 1H), 5.74 (dd, $J$ = 9.9, 3.9 Hz, 1H), 5.58 (dd, $J$ = 10.0, 4.0 Hz, 1H), 2.29 (s, 3H), 2.08 (s, 3H). ^{13}C NMR (101 MHz, CDCl$_3$) $\delta$ 172.6, 163.8, 162.6, 162.2, 161.9, 161.3, 160.6, 160.4, 159.7, 158.6, 151.0, 148.4, 148.1, 147.7, 139.5, 138.8, 134.3, 134.1, 133.8, 133.3, 133.0, 132.7, 132.2, 130.7, 129.7, 128.5, 123.6, 123.4, 123.1, 115.8, 18.4, 18.3. HRMS (MALDI-TOF, $m/z$): calcd. for C$_{54}$H$_{38}$F$_4$IrN$_3$O$_4$P$_2$ 1123.1903, found 1124.1914 ([M+H]$^+$), 1146.1789 ([M+Na]$^+$), 1162.1595 ([M+K]$^+$).

**Ir3**. Yield: 45%; a yellow solid. $^1$H NMR (400 MHz, CDCl$_3$) $\delta$ 8.98 (s, 1H), 8.39 (d, $J$ = 7.7 Hz, 1H), 8.28 (t, $J$ = 10.2 Hz, 2H), 8.09 (td, $J$ = 7.7, 1.2 Hz, 1H), 8.01 - 7.88 (m, 2H), 7.88 - 7.64 (m, 9H), 7.65 - 7.31 (m, 14H), 5.75 (dd, $J$ = 9.5, 3.7 Hz, 1H), 5.57 (dd, $J$ = 9.6, 3.7 Hz, 1H). $^{13}$C NMR (101 MHz, CDCl$_3$): $\delta$ 171.9, 168.1, 166.8, 165.3, 165.0, 164.4, 164.1, 162.6, 162.4, 161.9, 161.4, 160.4, 159.4, 150.7, 148.5, 136.2, 132.2, 132.0, 131.1, 129.4, 129.2, 128.9, 128.8, 128.7, 128.6, 120.4, 120.3, 116.1, 105.0, 104.0. HRMS (MALDI-TOF, $m/z$): calcd. for C$_{54}$H$_{32}$F$_{10}$IrN$_3$O$_4$P$_2$ 1231.1338, found 1232.1458 ([M+H]$^+$), 1254.1292 ([M+Na]$^+$).
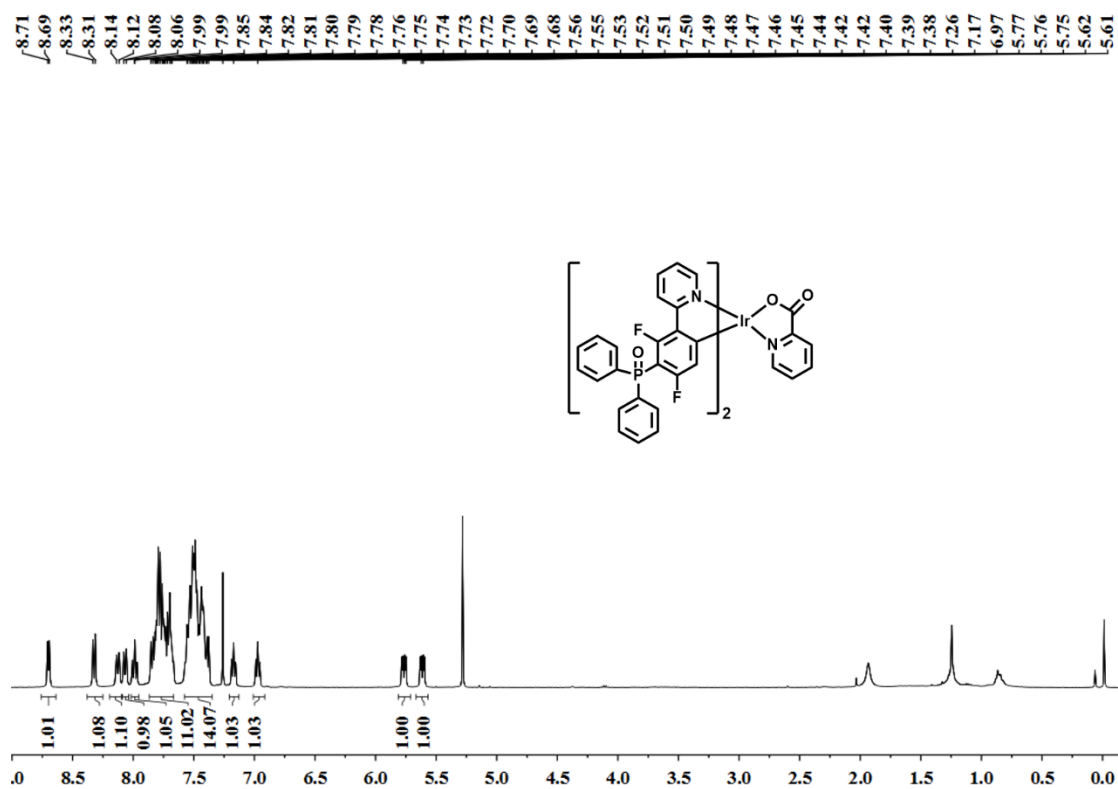
**Figure S1.** The $^1$H NMR spectrum of **Ir1** in CDCl$_3$.
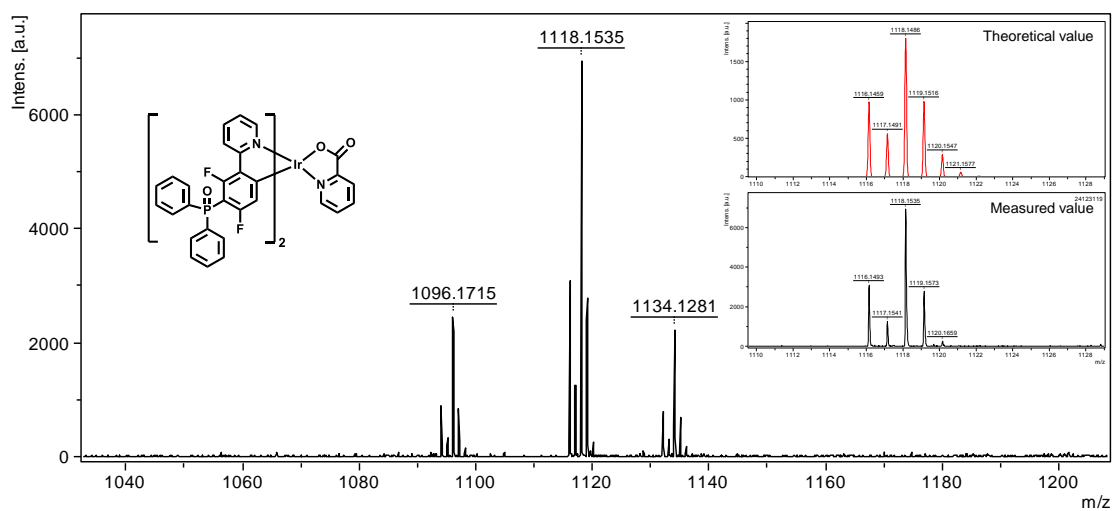


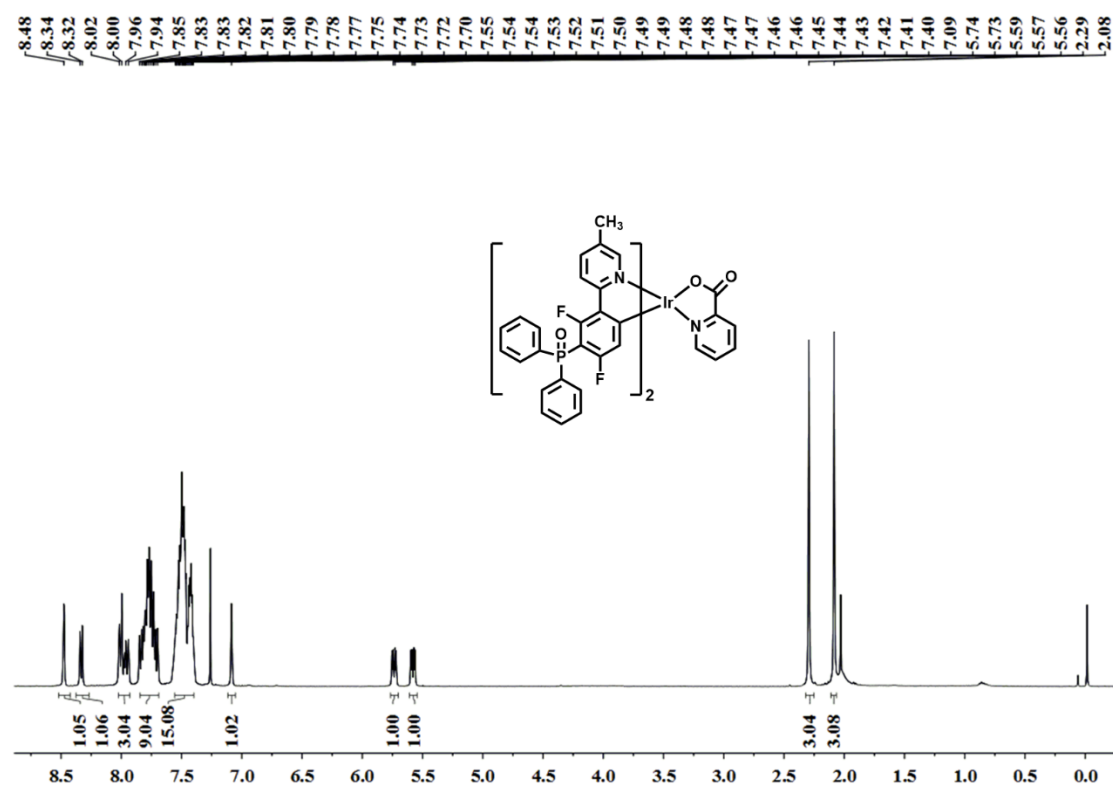**Figure S2.** The HRMS of **Ir1**. Inset: Theoretical (top) and high-resolution mass spectra (bottom) of **Ir1**.

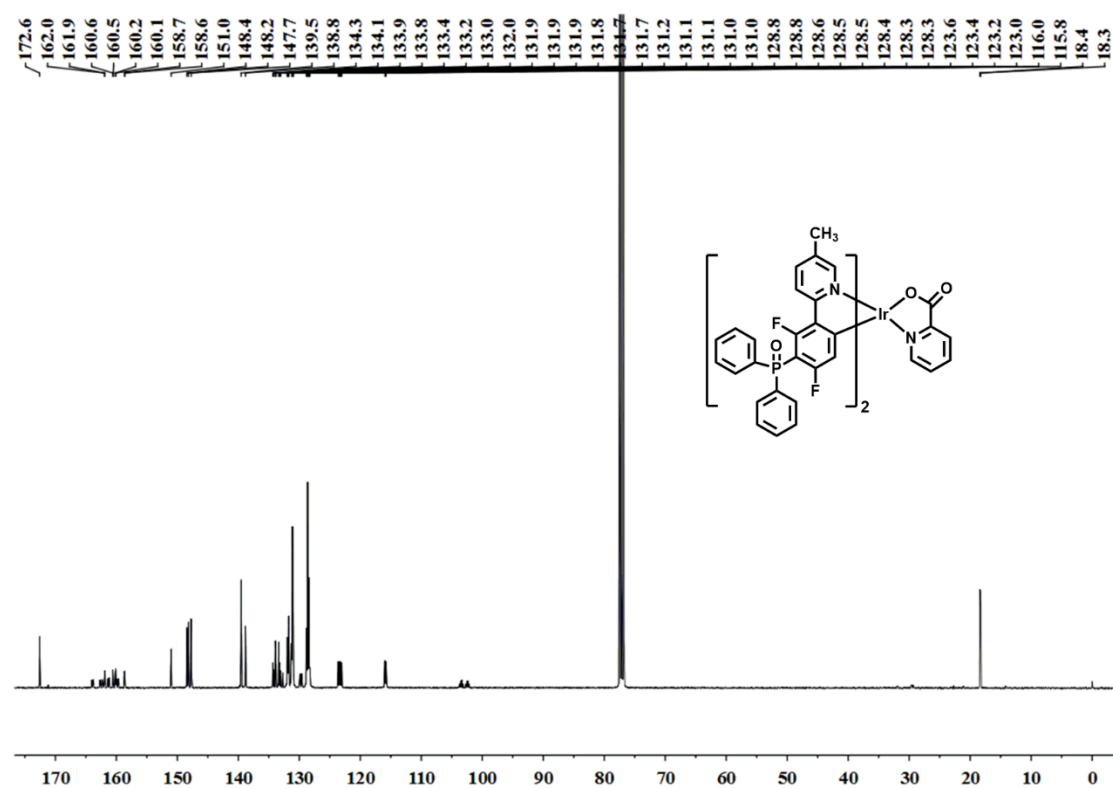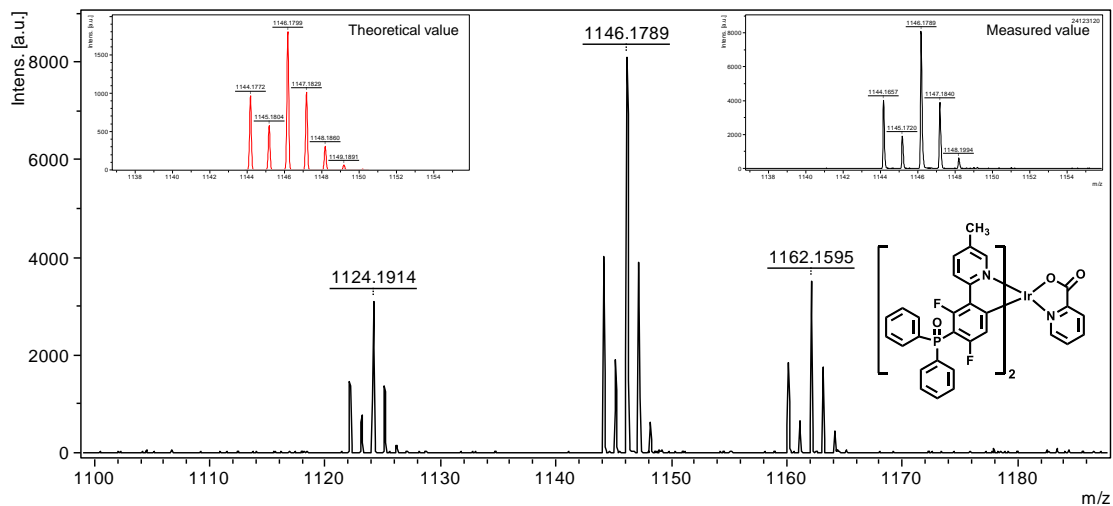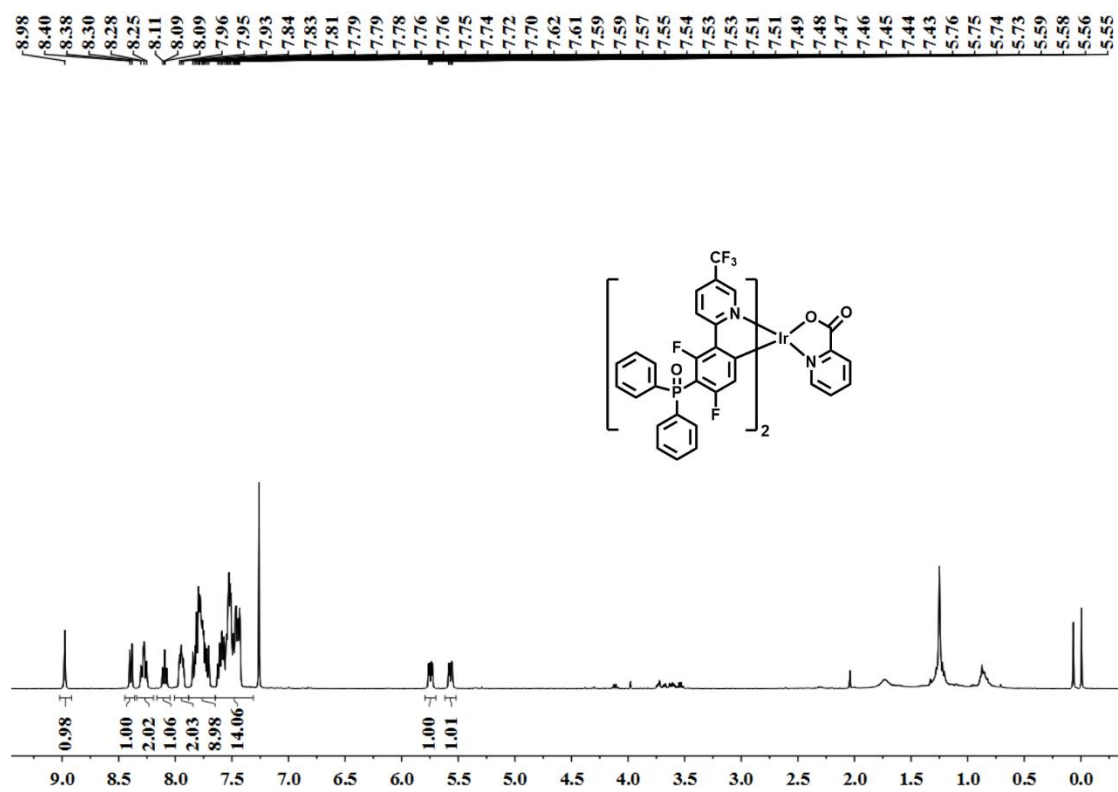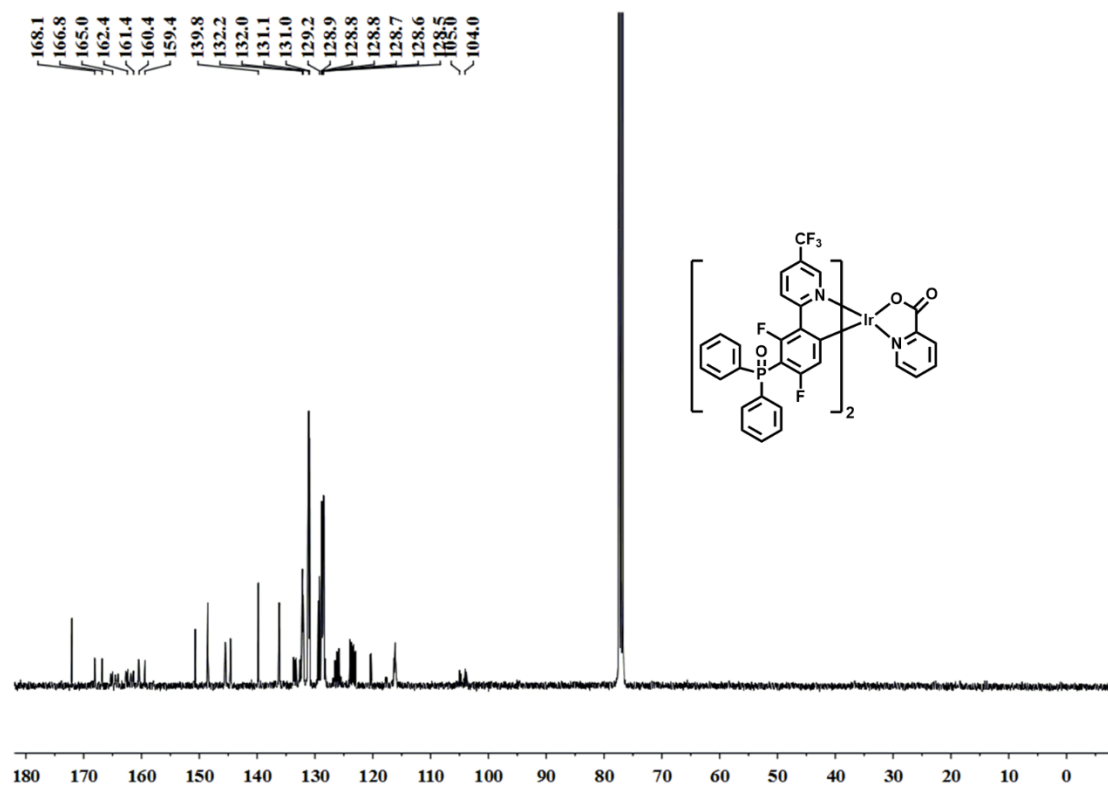**Figure S3.** The $^1$H NMR spectrum of **Ir2** in CDCl$_3$.



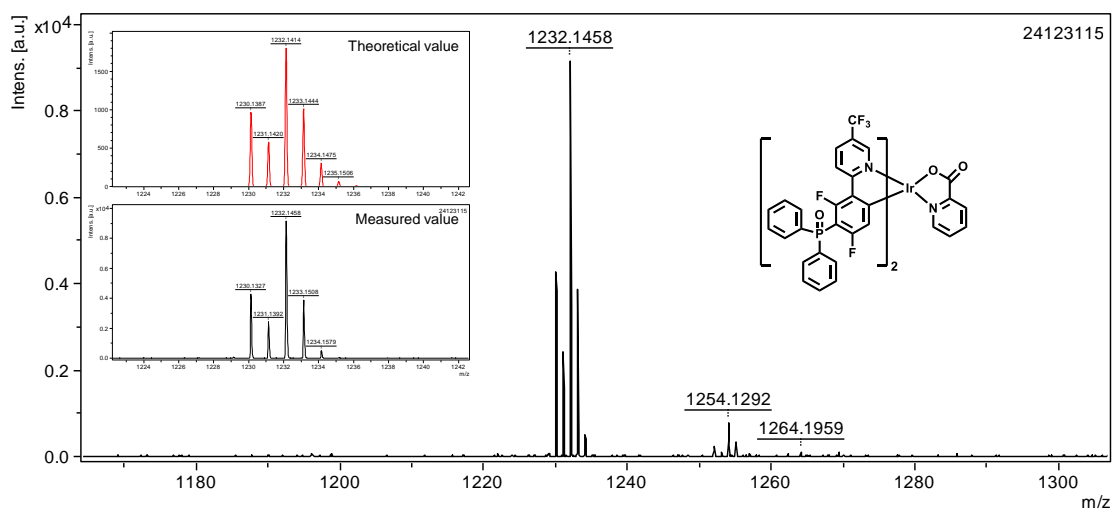**Figure S4.** The $^{13}$C NMR spectrum of **Ir2** in CDCl$_3$.

**Figure S5.** The HRMS of **Ir2**. Inset: Theoretical (left) and high-resolution mass spectra (right) of **Ir2**.
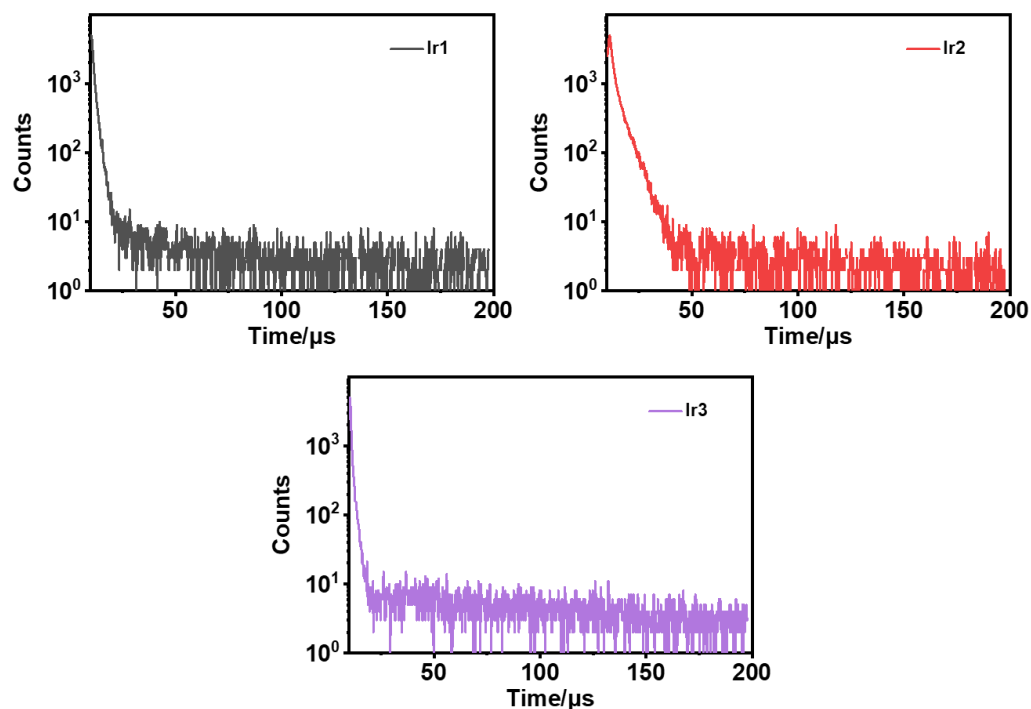


**Figure S6.** The $^1$H NMR spectrum of **Ir3** in CDCl$_3$.

**Figure S7.** The $^{13}$C NMR spectrum of **Ir3** in CDCl$_3$.



**Figure S8.** The HRMS of **Ir3**. Inset: Theoretical (top) and high-resolution mass spectra (bottom) of **Ir3**.

**Photophysical Properties**



**Figure S9.** Phosphorescence decay traces of **Ir1-Ir3** in deoxygenated $CH_2Cl_2$.

**Table S1.** Photophysical data of **Ir1-Ir3**.

| Complexes | $\lambda_{abs}{}^{a}$ (nm) | $\lambda_{em}{}^{b}$ (nm) | $\Phi_{PL}{}^{c}$ | $\tau^{d}$ (µs) |
|---|---|---|---|---|
| **Ir1** | 235 (0.48), 260 (0.55), 375 (0.056) | **462**, 487 | 0.69 | 1.32 |
| **Ir2** | 235 (0.49), 260 (0.61), 375 (0.062) | **465**, 491 | 0.70 | 3.32 |
| **Ir3** | 235 (0.40), 265 (0.54), 290 (0.45), 380 (0.039) | **490** | 0.72 | 1.01 |

[a] Measured in THF at a concentration of $10^{-5}$ M, with extinction coefficients ($10^5$ $M^{-1}$ $cm^{-1}$) shown in parentheses. [b] The emission maxima of the complexes in THF are the values in bold. [c] The quantum yields ($\Phi_{solution}$) in deoxygenated $CH_2Cl_2$ were measured with [Ir(ppy)$_2$(acac)] ($\Phi_{PL}=0.34$) as a standard. [d] In deoxygenated $CH_2Cl_2$ solution.

**DLS Analysis of Ir1**
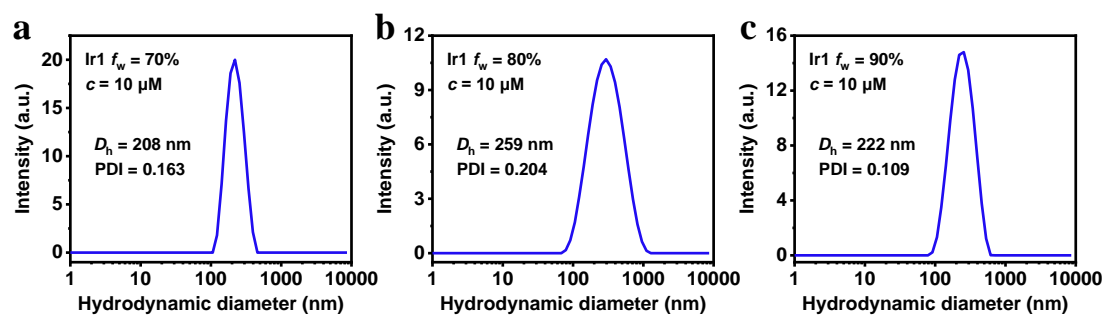
**Figure S10.** DLS analysis of **Ir1** at 70% (a), 80% (b), and 90% (c) water fractions (10 μM, $H_2O$/THF).

**PA Detection of Ir1-Ir3**

The limits of detection of **Ir1-Ir3** were calculated according to the following equation: LOD = $3\sigma/K$, where $\sigma$ represents the standard deviation of the blank measurement and $K$ represents the slope of the linear relationship between the emission intensity $I$ and the PA concentration.
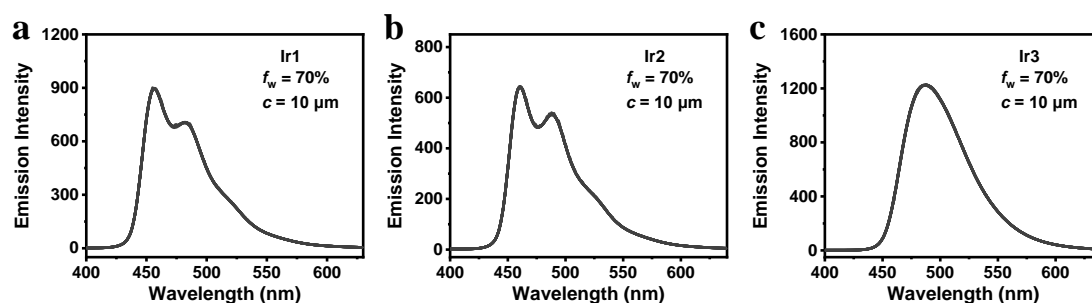


**Figure S11.** The emission spectra of **Ir1** (a), **Ir2** (b), and **Ir3** (c) in $H_2O$/THF (v/v = 7:3, 10 μM) at eleven time points (blank measurement). The excitation wavelength was 330 nm.

**Table S2** The emission intensities of **Ir1** at 456 nm, **Ir2** at 461 nm, and **Ir3** at 488 nm at eleven time points in $H_2O$/THF (v/v = 7:3, 10 μM)

| Complexes | Ir1 | Ir2 | Ir3 |
|---|---|---|---|
| $X_1$ | 896.53 | 642.38 | 1225.30 |
| $X_2$ | 896.41 | 642.29 | 1225.40 |
| $X_3$ | 896.29 | 642.52 | 1224.50 |
| $X_4$ | 896.66 | 642.56 | 1224.50 |
| $X_5$ | 896.67 | 643.52 | 1226.30 |
| $X_6$ | 896.74 | 643.15 | 1225.00 |
| $X_7$ | 896.56 | 642.22 | 1225.60 |
| $X_8$ | 896.00 | 642.79 | 1226.30 |
| $X_9$ | 895.32 | 642.88 | 1224.80 |
| $X_{10}$ | 895.94 | 642.98 | 1226.10 |
| $X_{11}$ | 895.70 | 643.43 | 1225.70 |
| X | 896.26 | 642.79 | 1225.41 |

The values of $\sigma$ for **Ir1-Ir3** were calculated according to the following equation:

$$\sigma = [\ \sum(X_i - X)^2\ /\ (n-1)\ ]^{0.5}$$

$X_i$ (i = 1, 2, 3...11) represents the emission intensity of each test, X represents the mean value of the emission intensity, and n represent the number of tests.

According to the above formula, the values of $\sigma$ for **Ir1-Ir3** were calculated to be 0.44, 0.42, and 0.63, respectively.
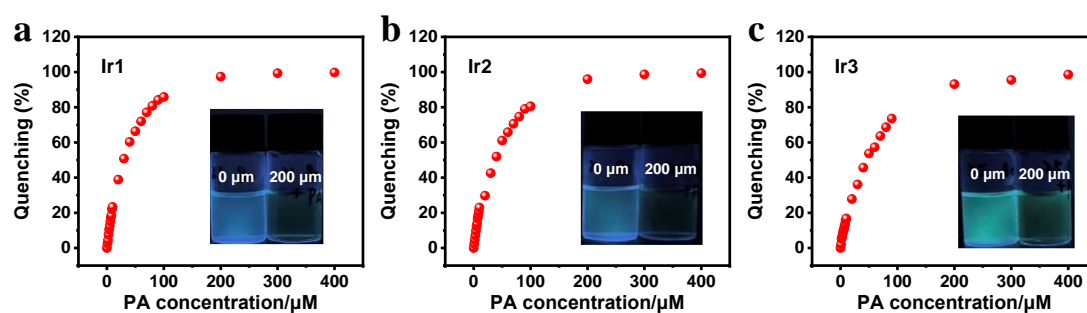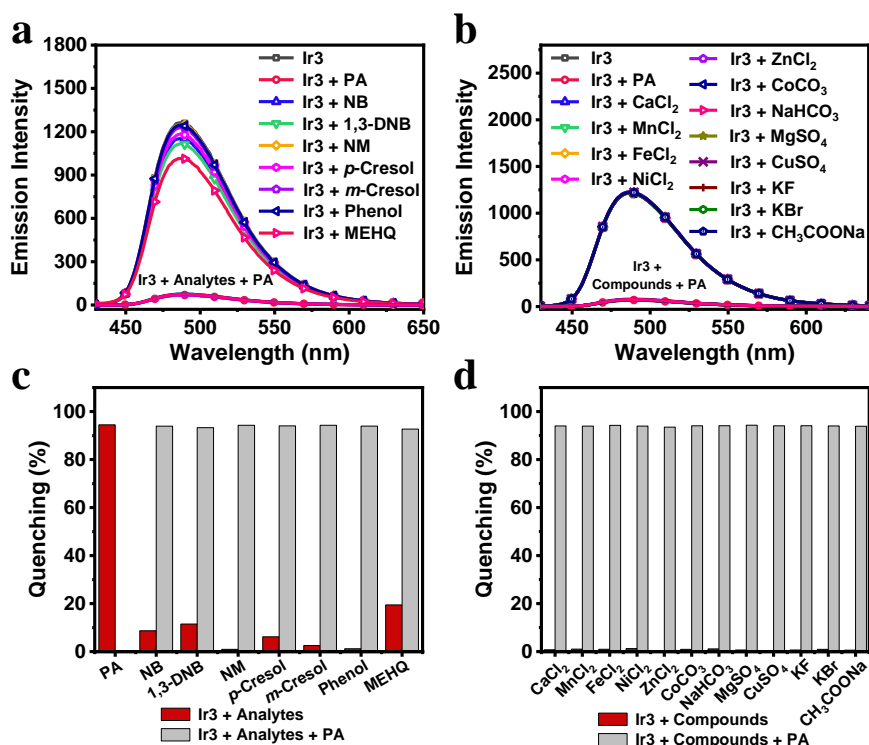


**Figure S12.** Quenching percentages of **Ir1** (a), **Ir2** (b), and **Ir3** (c) after adding PA at various concentrations. Insert: Photos of **Ir1-Ir3** at PA concentrations of 0 and 200 μM under 365 nm UV light.
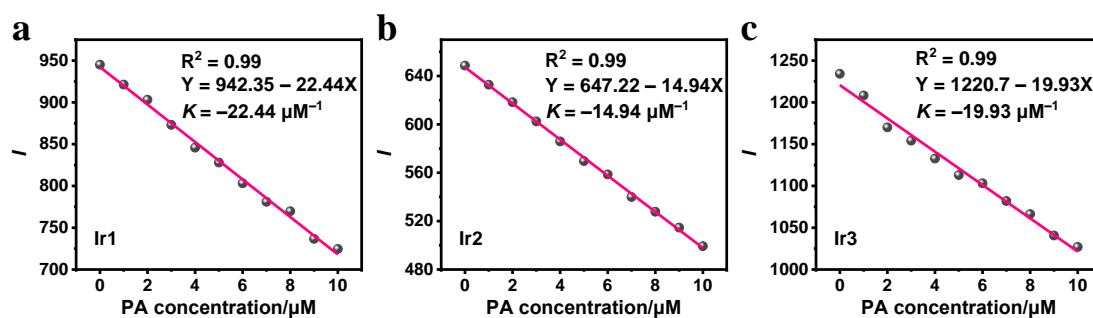


**Figure S13.** The linear graphs of the emission intensities of **Ir1** (a), **Ir2** (b), and **Ir3** (c) vs. the concentration of PA.
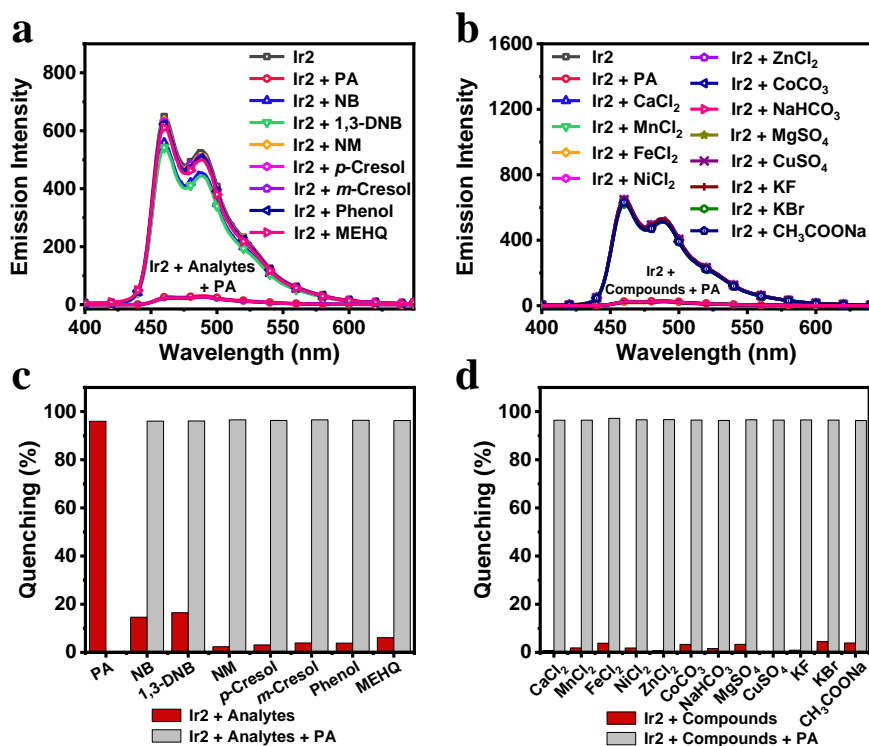
**Figure S14.** The emission spectra of **Ir2** in $H_2O$/THF (v/v = 7:3, 10 μM) with different analytes (a) and ionic compounds (b) present. The excitation wavelength was 330 nm. Quenching percentages of **Ir2** with different analytes (c) and ionic compounds (d) before (red) and after (gray) the addition of PA.



**Figure S15.** The emission spectra of **Ir3** in $H_2O$/THF (v/v = 7:3, 10 μM) with different analytes (a) and ionic compounds (b) present. The excitation wavelength was 330 nm. Quenching percentages of **Ir3** with different analytes (c) and ionic compounds (d) before (red) and after (gray) the addition of PA.
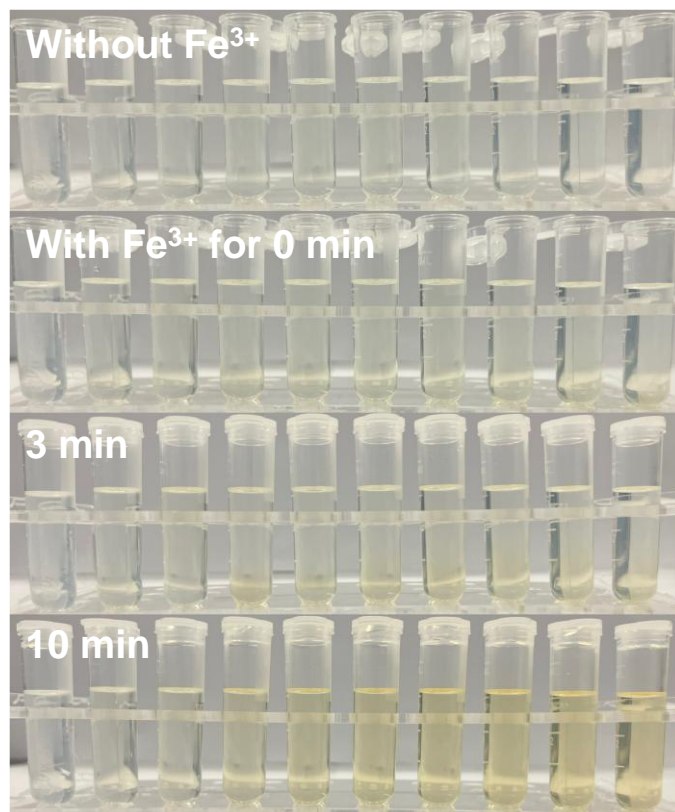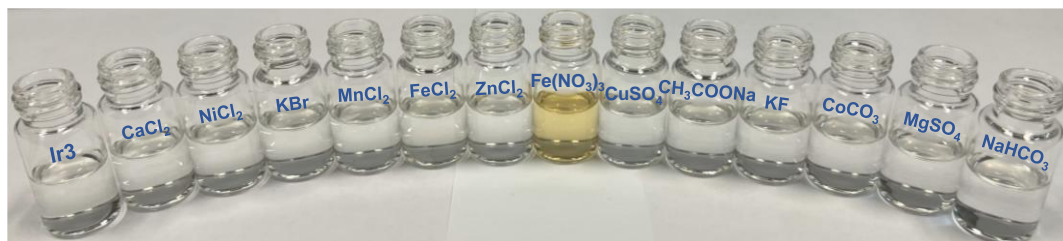
**Fe$^{3+}$ Detection of Ir1-Ir3**
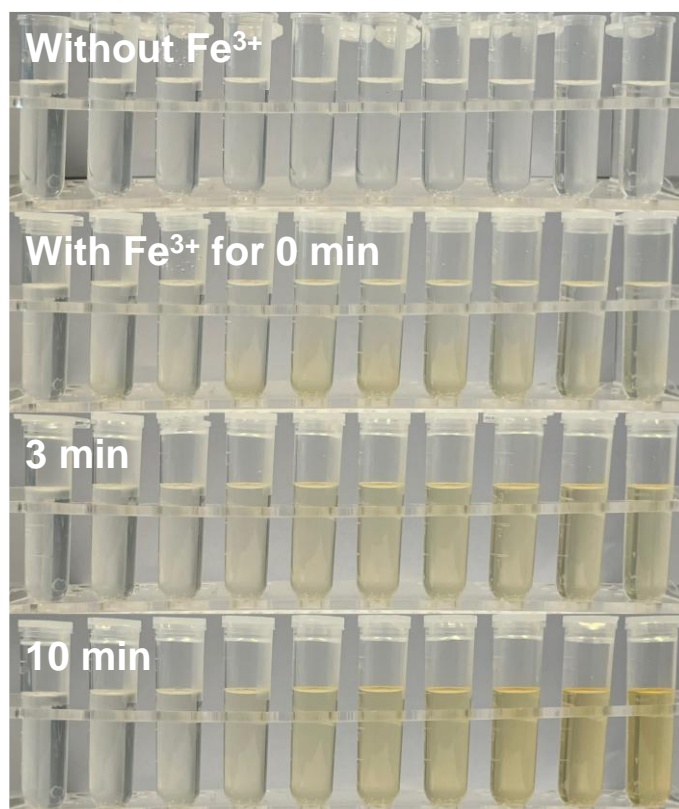


**Figure S16.** The color change in **Ir1** in H$_2$O/THF in the presence of Fe$^{3+}$ at different concentrations. The Fe$^{3+}$ concentrations are 0, 50, 100, 200, 300, 400, 500, 600, 700, and 800 μM from left to right, respectively.
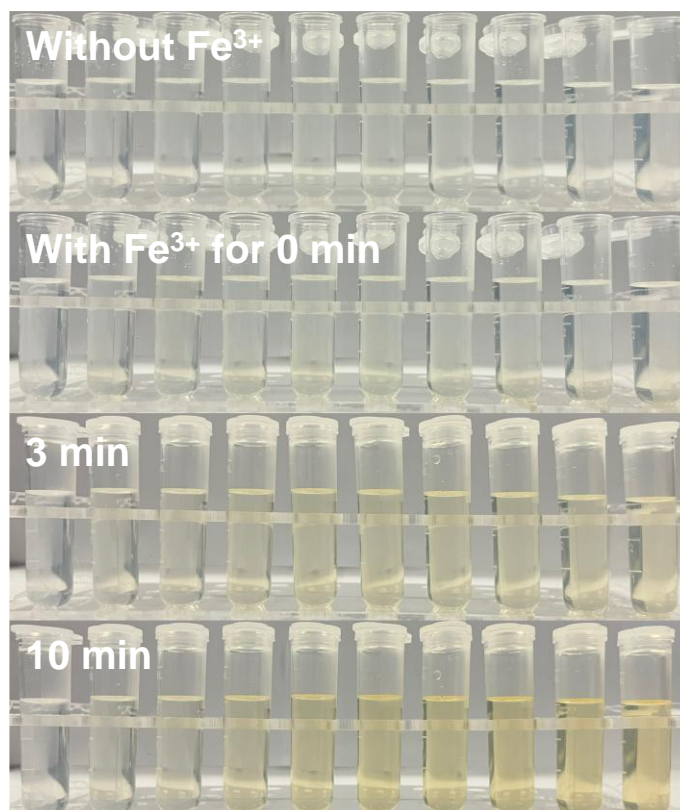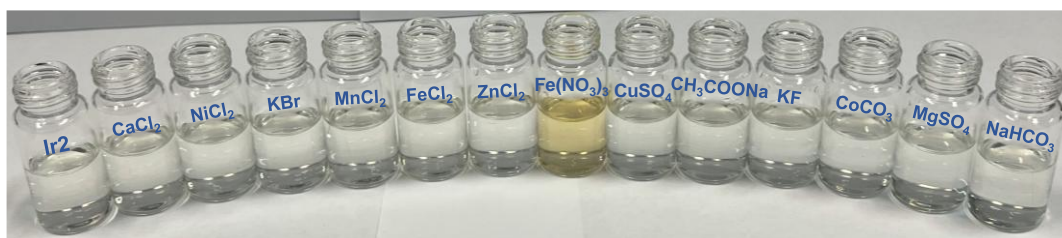
**Figure S17.** (a) The color change in **Ir2** in $H_2O$/THF in the presence of $Fe^{3+}$ at different concentrations. The $Fe^{3+}$ concentrations are 0, 50, 100, 200, 300, 400, 500, 600, 700, and 800 μM from left to right, respectively. (b) The color of **Ir2** in $H_2O$/THF in the presence of various ionic compounds.

**Figure S18.** (a) The color change in **Ir3** in $H_2O$/THF in the presence of $Fe^{3+}$ at different concentrations. The $Fe^{3+}$ concentrations are 0, 50, 100, 200, 300, 400, 500, 600, 700, and 800 μM from left to right, respectively. (b) The color of **Ir3** in $H_2O$/THF in the presence of various ionic compounds.
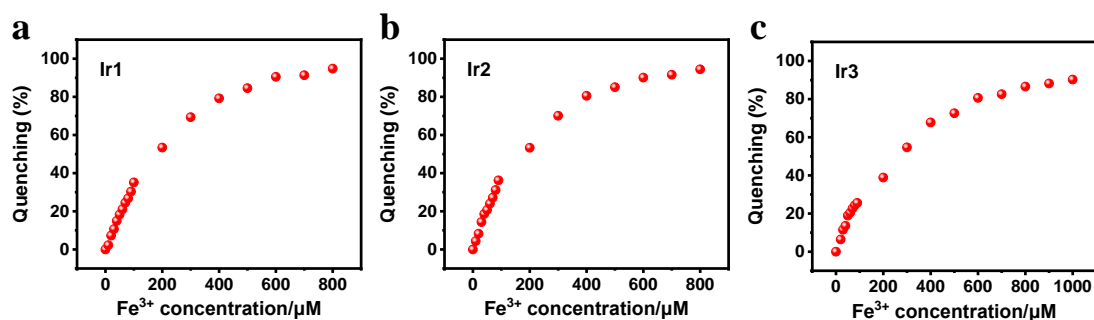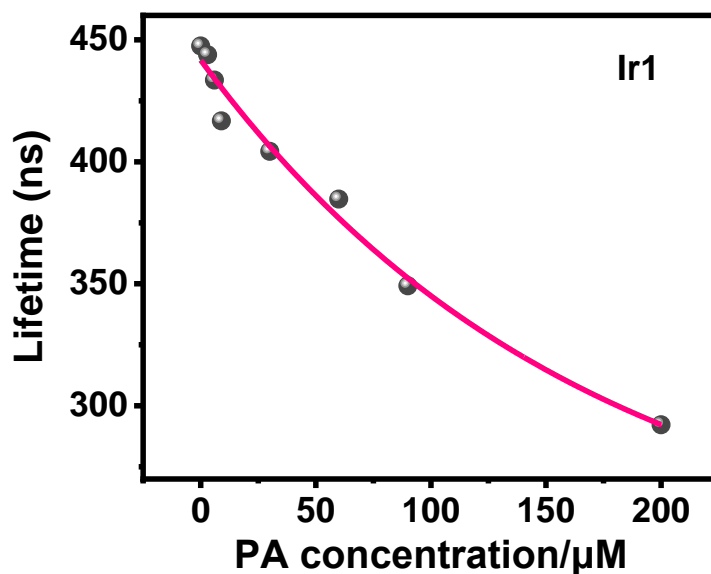
**Figure S19.** Quenching percentages of **Ir1** (a), **Ir2** (b), and **Ir3** (c) after adding $Fe^{3+}$ at various concentrations.
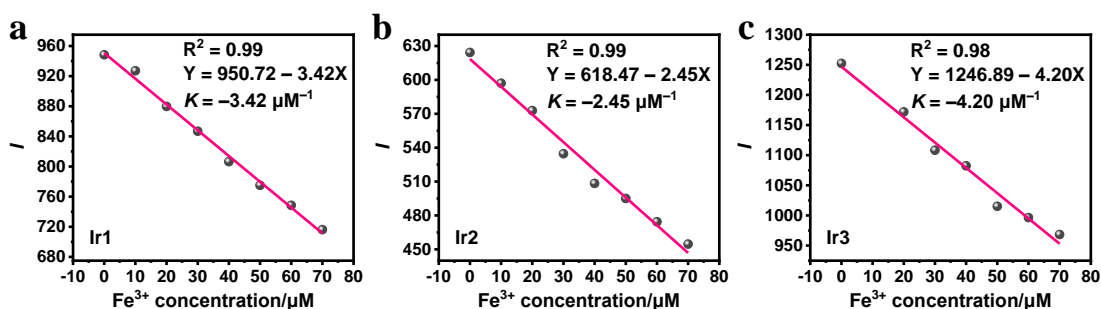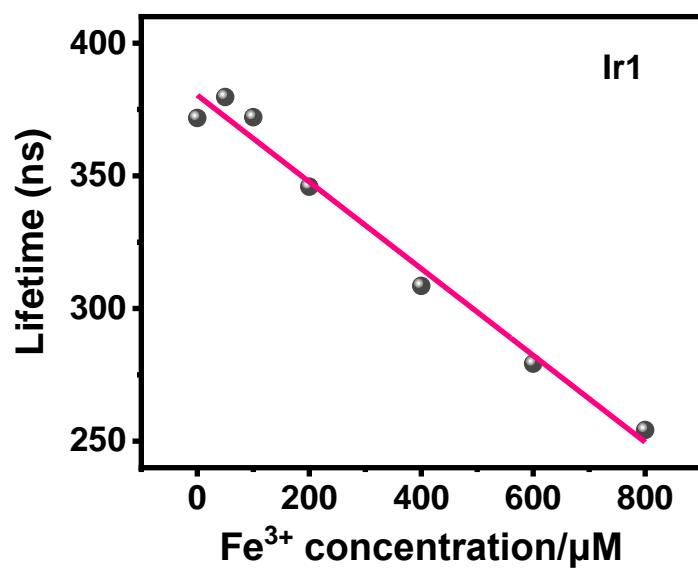


**Figure S20.** The linear graphs of the emission intensities of **Ir1** (a), **Ir2** (b), and **Ir3** (c) vs. the concentration of $Fe^{3+}$.



**Figure S21.** Lifetimes of **Ir1** in $H_2O$/THF (v/v = 7:3, 10 μM) after the addition of PA at different concentrations.

**Figure S22.** Lifetimes of **Ir1** in $H_2O$/THF (v/v = 7:3, 10 μM) after the addition of $Fe^{3+}$ at different concentrations.

## References

[1] Yu, H.; Liu, C.; Lv, X.; Xiu, J.; Zhao, J. Effect of substituents on properties of diphenylphosphoryl-substituted bis-cyclometalated Ir(III) complexes with a picolinic acid as ancillary ligand. *Dyes Pigm.* **2017**, *145*, 136-143.